Land subsidence of natural transitional environments by satellite radar interferometry on artificial reflectors

Tazio Strozzi,[1] Pietro Teatini,[2,3] Luigi Tosi,[2] Urs Wegmüller,[1] and Charles Werner[1]

Received 6 November 2012; revised 14 May 2013; accepted 17 May 2013.

[1] Land subsidence is a widespread phenomenon, particularly relevant to transitional environments, such as wetlands, deltas, and lagoons, characterized by low elevation with respect to the mean sea level. Satellite synthetic aperture radar (SAR) interferometry offers the possibility to effectively and precisely measure land displacements for dry surfaces or anthropogenic structures, but difficulties arise in identifying long-term stable targets in natural transitional regions. In order to improve the coverage of satellite SAR interferometry in salt marshes within the Venice Lagoon (Italy), we installed a network of 57 Trihedral Corner Reflectors (TCRs). The TCRs were monitored by ENVISAT ASAR and TerraSAR-X acquisitions covering the time period from November 2006 to September 2011. The results show that the northern lagoon basin is subsiding at ~3 mm/yr and that the central and southern portions are more stable. Larger subsidence rates, up to 6 mm/yr, are measured where surficial loads, such as artificial salt marshes or embankments, rise above the lagoon bottom. The accuracy of TerraSAR-X is greater than ENVISAT due to the shorter wavelength and higher spatial resolution in relationship to the size of the TCRs. The observations obtained in the Venice Lagoon indicate that SAR interferometry using a large network of artificial reflectors is an effective and powerful methodology to monitor land subsidence in transitional environments where the loss of elevation with respect to the mean sea level can yield significant morphological changes to the natural environment.

Citation: Strozzi, T., P. Teatini, L. Tosi, U. Wegmüller, and C. Werner (2013), Land subsidence of natural transitional environments by satellite radar interferometry on artificial reflectors, *J. Geophys. Res. Earth Surf.*, *118*, doi:10.1002/jgrf.20082.

1. Introduction

[2] The persistent scatterer approach in satellite synthetic aperture radar (SAR) interferometry Persistent, Scatterer and Interferometry (PSI) has recently produced impressive results in the monitoring of ground surface displacements over large plain areas. The movements due to aquifer pumping and recharge [e.g., *Bell et al*., 2008], development of gas reservoirs [e.g., *Ketelaar*, 2009], natural consolidation of Holocene and Quaternary deposits [e.g., *Teatini et al*., 2011a], geological CO_2 sequestration [e.g., *Vasco et al*., 2010], CH_4 storage in depleted gas fields [*Teatini et al*., 2011b], and fault activation and fissure generation [e.g., *Bürgmann et al*., 2006] have been detected with a resolution impossible to acquire by leveling and GPS. The key to the PSI approach is the identification and exploitation of time coherent radar reflectors [*Ferretti et al*., 2001; *Werner et al*., 2003]. These scatterers typically are man-made structures within the landscape, such as buildings, utility poles, roadways, or natural features, such as rocks, deserts with little shifting sand, or saline soils. A potentially severe limitation of PSI is the difficulty of identifying stable targets in rural and agricultural areas.

[3] The lack of radar reflectors, or their location at a distance from one to another too large to reliably resolve the radar phase ambiguities in the presence of atmospheric artifacts, characterizes many natural environments, such as deltas, wetlands, and lagoons. The use of PSI to monitor displacements in these environments is thus very limited or totally precluded. Unfortunately, these coastal zones are the most vulnerable to land subsidence due to their low elevation with respect to the mean sea level, the diminishing supply of new sediments caused by trapping in the upland drainage basins, and mean sea level raise due to climate changes [*Syvitski et al*., 2009]. The quantification of subsidence is usually carried out by leveling and GPS [e.g., *Morton and Bernier*, 2010]. Performing ground campaigns in these areas characterized by marshlands, tidal marshes, channels, and ponds is however both time-consuming and costly due to lack of accessibility.

[4] *Coulson and Guignard* [1994] and *Ge et al*. [2001] have demonstrated that artificial passive reflectors could be used to detect displacements with satellite SAR interferometry. Their application, however, was restricted to very few reflectors with the main aim of calibrating the SAR-based methodology or monitoring the movements of restricted

[1]Gamma Remote Sensing, Gümligen, Switzerland.
[2]Institute of Marine Sciences, National Research Council, Venezia, Italy.
[3]Department of Civil Environmental and Architectural Engineering, University of Padova, Padova, Italy.

Corresponding author: T. Strozzi, Gamma Remote Sensing, Worbstrasse 225, Gümligen, BE 3073, Switzerland. (strozzi@gamma-rs.ch)

2169-9003/13/10.1002/jgrf.20082

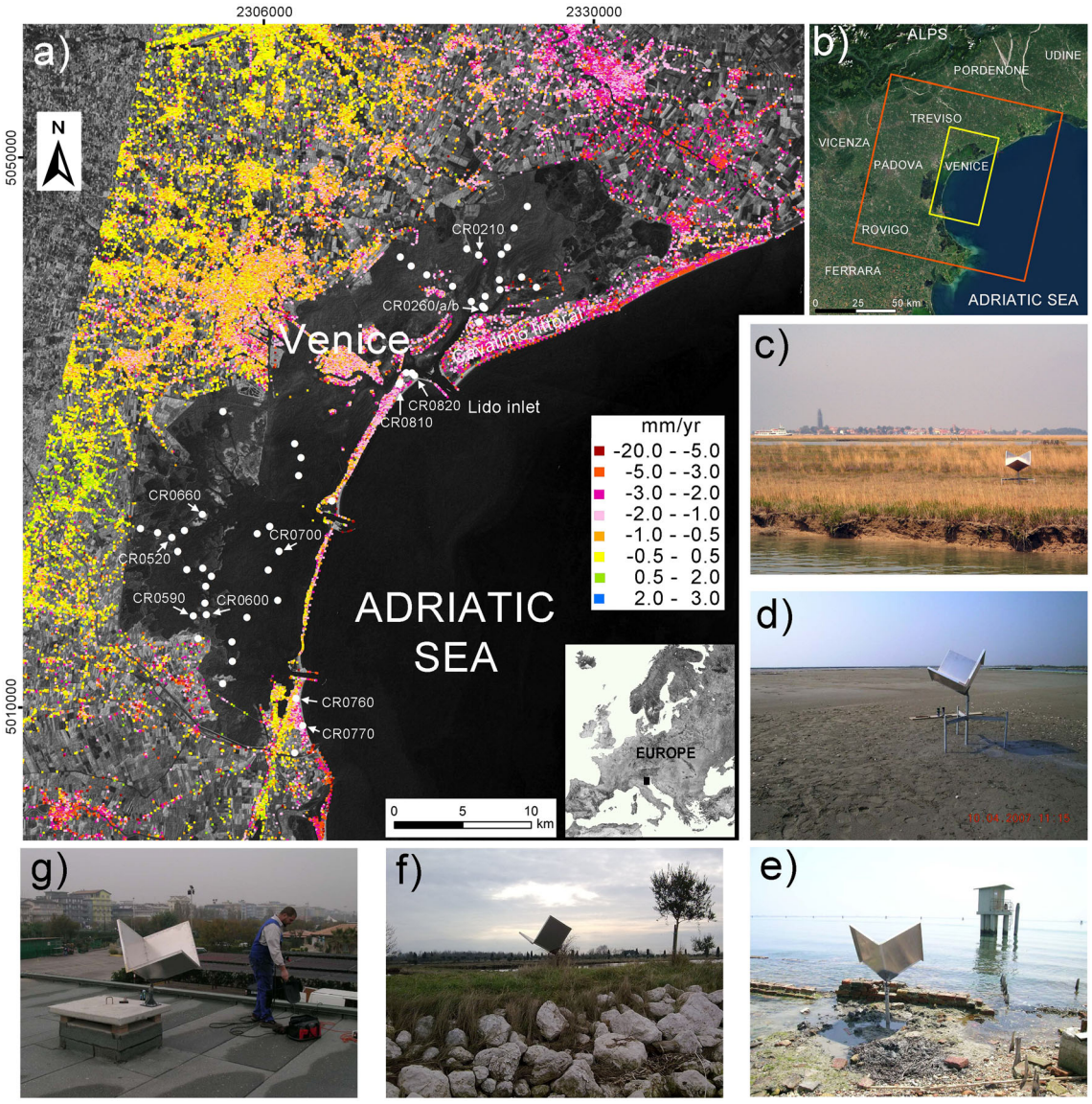

Figure 1. (a) Landsat image of the Venice Lagoon, Italy, with the velocity map obtained by PSI from ENVISAT ASAR data for the period 2003–2010 and the network of TCRs. Movements are in the satellite LOS direction, negative values indicate settlement, positive mean uplift. The labeled TCRs are those that are further discussed in the paper. (b) Footprints of the ENVISAT ASAR (path 122, frame 2691, red box) and TerraSAR-X (beam strip_006R, yellow box) frames. The photos of a few TCRs representative of the various lagoon environments, i.e., (c) natural and (d) artificial tidal marshes, small islands corresponding to (e) ancient sandy coastal ridges, (f) artificial embankments, and (g) urban zones, are provided in the insets.

zones. An experiment was carried out by *Marinkovic et al.* [2004, 2008] in Delft, The Netherlands, to monitor a set of artificial reflectors where the phase histories were validated by additional measurements. Five corner reflectors were deployed at a relative distance of 150 m, and during every ERS-2 and ENVISAT SAR satellite acquisition, these reflectors were leveled with millimeter precision. Two pairs of dihedral reflectors, approximately 50 m apart to reduce the impact of the atmospheric effects on the phase values, were used by *Ferretti et al.* [2007] to demonstrate that SAR measurements with ENVISAT ASAR and RADARSAT-1 data permit generation of displacement time series with submillimeter accuracy both in the horizontal and vertical directions. Networks of about 10 corner reflectors were established by *Xia et al.* [2002, 2004] and *Fu et al.* [2010] in order to monitor the stability of ~1 km long landslides in regions of low coherence along the banks of the Yangtze River in the Three Gorges area with ERS-2 and ENVISAT SAR scenes.

[5] We deployed a network of Trihedral Corner Reflectors (TCRs) to improve the SAR-derived estimates of subsidence in the Venice Lagoon, Italy (Figure 1a). The Venice Lagoon covers an area of about 550 km^2 and is a unique transitional environment vulnerable to loss in surface elevation because

Table 1. TCR List and Results[a]

TCR	Operation Period	Environment	Mean ENVISAT ASAR (mm/yr)	Standard Deviation ENVISAT ASAR (mm/yr)	Number of ENVISAT ASAR	Mean TerraSAR-X (mm/yr)	Standard Deviation TerraSAR-X (mm/yr)	Number of TerraSAR-X
CR0110	June 2007 – September 2009	natural marsh	2.032	3.27	16	−3.973	0.318	42
CR0150	June 2007 – December 2008	natural marsh	−0.169	2.461	16	−2.202	0.854	25
CR0160	since December 2006	fish-farm embankment	−3.131	0.305	40	−3.78	0.041	90
CR0170	since March 2007	natural marsh	−1.528	0.578	38	−3.206	0.04	90
CR0180	since June 2007	natural marsh	−1.071	0.615	35	−3.633	0.052	90
CR0190	since December 2006	natural marsh	−2.22	0.322	40	−3.616	0.02	90
CR0200	since January 2007	natural marsh	−1.224	0.319	39	−4.121	0.014	90
CR0210	since December 2006	island embankment	−6.797	0.916	40	−6.329	0.065	90
CR0230	since January 2007	natural marsh	−0.667	0.748	39	−1.361	0.047	90
CR0240	since April 2007	natural marsh	0.006	0.387	37	−1.653	0.064	90
CR0250	since January 2007	natural marsh	−1.152	0.55	39	−0.611	0.071	90
CR0260	since January 2007	natural marsh	−0.007	0.387	39	−0.822	0.07	90
CR0260a	since February 2008	natural marsh	−0.799	0.822	28	−0.399	0.085	90
CR0260b	since April 2008	natural marsh	−0.21	0.771	26	−0.729	0.099	87
CR0270	since May 2007	natural marsh	−0.191	0.316	36	−1.656	0.104	90
CR0280	September 2006 – April 2008	littoral strip	14.098	3.843	16	*−12.281*	*5.557*	*5*
CR0281	September 2006 – April 2008	littoral strip	−0.726	1.179	16	*80.565*	*4.098*	*5*
CR0290	since March 2007	natural marsh	−0.491	0.313	38	−1.575	0.102	90
CR0300	since March 2007	natural marsh	0.373	0.37	38	−1.189	0.121	90
CR0310	since March 2007	natural marsh	−0.175	0.285	38	−2.424	0.138	90
CR0320	since June 2007	natural marsh	−1.067	0.563	35	−2.101	0.081	90
CR0500	since January 2007	fish-farm embankment	0.982	0.573	39	–	–	–
CR0510	since January 2007	fish-farm embankment	−2.901	0.589	39	–	–	–
CR0520	since April 2007	fish-farm embankment	−6.989	0.575	37	–	–	–
CR0530	since March 2007	natural marsh	0.061	0.509	38	–	–	–
CR0540	since March 2007	natural marsh	0.265	0.564	38	–	–	–
CR0550	since March 2007	natural marsh	−0.102	0.633	38	–	–	–
CR0560	since June 2007	natural marsh	−0.818	0.748	35	–	–	–
CR0570	March 2007 – December 2009	natural marsh	−2.039	0.808	30	–	–	–
CR0580	December 2007 – December 2009	natural marsh	−0.086	1.156	22	–	–	–
CR0590	March 2007 – February2010	artificial marsh	−7.704	0.765	32	–	–	–
CR0600	since January 2007	natural marsh	−0.672	0.402	39	–	–	–
CR0610	since December 2010	inland infrastructure	−0.204	0.36	39	–	–	–
CR0620	June 2007 - June 2008	island	*4.956*	*3.963*	*10*	*−19.518*	*14.262*	*8*
CR0630	June 2007 – December 2008	island	1.62	1.452	16	−3.213	3.38	25
CR0640	April 2007 – June 2008	island	*0.112*	*2.051*	*12*	*−24.959*	*17.354*	*8*
CR0650	since June 2007	natural marsh	0.001	0.355	35	–	–	–
CR0660	since June 2007	artificial marsh	−3.277	0.765	35	–	–	–
CR0670	since June 2007	natural marsh	1.026	0.478	35	–	–	–
CR0680	since August 2008	island	−1.931	0.958	22	−1.659	0.362	75
CR0690	June 2007 – July 2008	island	0.218	2.548	12	−19.859	8.146	12
CR0700	since June 2007	island	−1.664	0.585	35	−3.096	0.468	75
CR0710	June 2007 – July 2010	island	−0.646	0.537	33	−1.732	0.506	61
CR0720	June 2007 – December 2008	island	3.095	0.957	16	−1.795	2.432	25
CR0730	June 2007 – December 2008	island	2.331	2.118	16	−0.264	3.072	25
CR0740	June 2007 – September 2007	natural marsh	*115.189*	*39.571*	*3*	–	–	–
CR0750	since December 2006	littoral strip	−0.519	0.197	41	0.503	0.254	90
CR0760	since December 2006	littoral strip	−2.388	0.341	41	−2.578	0.182	90
CR0770	December 2006 – December 2009	littoral strip	−1.957	0.44	31	−3.539	0.151	43

Table 1. (continued)

TCR	Operation Period	Environment	Mean ENVISAT ASAR (mm/yr)	Standard Deviation ENVISAT ASAR (mm/yr)	Number of ENVISAT ASAR	Mean TerraSAR-X (mm/yr)	Standard Deviation TerraSAR-X (mm/yr)	Number of TerraSAR-X
CR0780	June 2007 – February2010	island	−0.873	0.485	29	−0.223	0.794	52
CR0790	December 2007 – March 2008	littoral strip	*−0.23*	*1.157*	*12*	–	–	–
CR0800	since August 2006	natural marsh	1.223	0.556	43	−1.056	0.25	90
CR0810	since May 2007	littoral strip	−0.527	0.201	36	−0.619	0.185	90
CR0820	since May 2007	littoral strip	−2.097	0.651	36	−0.468	0.111	90
CR0830	since May 2007	littoral strip	0.148	0.366	36	2.358	0.152	90
CR0840	since May 2007	littoral strip	−1.88	0.363	36	−1.506	0.229	82
CR0850	since May 2007	littoral strip	−0.472	0.523	36	−1.384	0.167	90

[a]Mean displacement rates in the LOS direction, standard deviation, and number of valid acquisitions of the TCRs using ENVISAT ASAR and TerraSAR-X data. Reflectors in the western side of the southern lagoon are not within the TerraSAR-X frame. Text in italic highlights the TRC with less than 16 acquisitions. The operation period and the environment where the TCRs were established are also provided.

of land subsidence and eustasy [*Carbognin et al*., 2004, 2010]. Land displacement in the Venice coastal zone has been determined over time by spirit leveling and GPS. Recently, SAR interferometry has been used to complement the ground-based methods [*Tosi et al*., 2002]. In particular, interferometric analysis on persistent Point Targets (PTs) was found to be very effective in detecting land displacement in this coastal environment. ERS [*Teatini et al*., 2005; *Teatini et al*., 2007] and ENVISAT [*Tosi et al*., 2010; *Teatini et al*., 2012] SAR images of the time periods 1992–2005 and 2003–2007, respectively, were analyzed at regional and local scale and has allowed quantifying the vertical displacements of thousands of PTs scattered on the mainland, the urbanized islands, the lagoon margins, and the littorals (Figure 1a). At regional scale, the central lagoon, including the city of Venice, shows a general stability, while the northern and southern lagoon extremities and their related catchment sectors sink with rates averaging 3–10 mm/yr. The observed land displacements were associated with geological features of the study region, including tectonics, seismicity, differential consolidation of the middle upper Pleistocene and Holocene deposits, and anthropogenic activities, such as land reclamation and groundwater withdrawal [*Teatini et al*., 2007; *Tosi et al*., 2009]. Local subsidence on the order of a few centimeters was detected by PSI on TerraSAR-X scenes at the three inlets connecting the Adriatic Sea to the lagoon [*Strozzi et al*., 2009], where major construction is under way to disconnect the inner water body from the sea by a series of mobile barriers.

[6] However, no information was retrieved in salt marshes and tidal flats within the inner lagoon where anthropogenic structures are completely lacking or are too sparsely distributed in order to reliably resolve the radar phase ambiguity in the presence of atmospheric disturbances. An accurate quantification of land subsidence within the inner lagoon assumes a strategic importance in relation to a general degradation that the lagoon has been experiencing over the last century consisting of the deepening of tidal flats and the reduction of salt marshes [*Carniello et al*., 2009]. Because also traditional monitoring techniques are not feasible in these zones, a research project was initiated by the Venice Water Authority to establish a network of TCRs for improving the PSI coverage in the lagoon environment. We present the results of this activity in this paper as follows. First, the network of TCRs established in the Venice Lagoon is described. Second, the SAR methodology on TCRs is discussed, showing the steps developed to improve the PSI result on these targets and to include the TCR-based solution into the global interferometric point target analysis on natural targets. Third, the quality of the measurements is assessed. Then, the results are shown with a comparison of the data from ENVISAT ASAR and TerraSAR-X. Finally, an interpretation of the detected displacements is provided in the light of present-day knowledge of the geomorphological features of the lagoon and of natural and anthropogenic processes impacting on the stability of the area.

2. Network of Trihedral Corner Reflectors (TCRs)

[7] Between November 2006 and July 2007, a network of 57 TCRs was installed on natural and rebuilt marshes, small

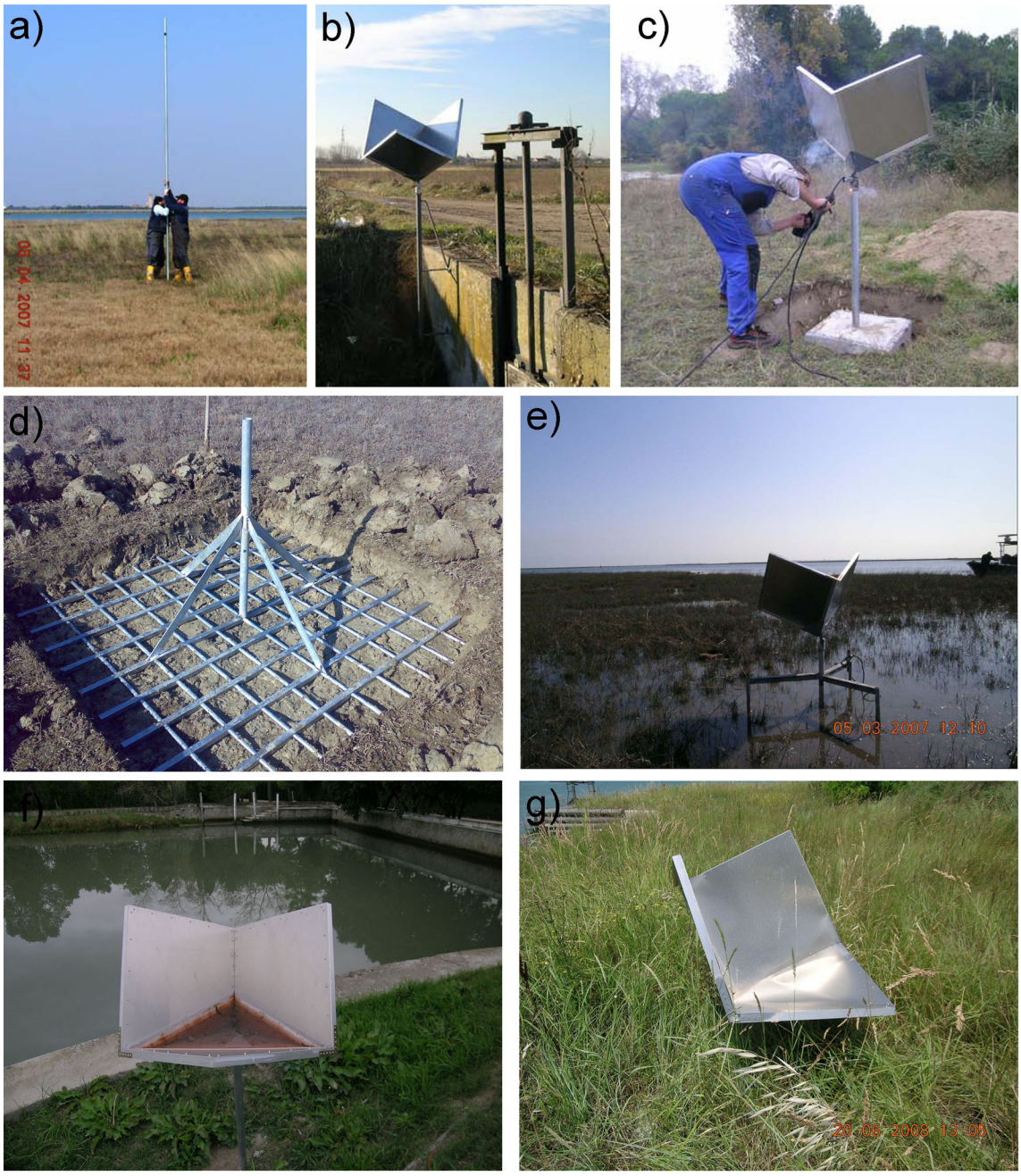

Figure 2. Photographs of various types of TCRs foundations used in the Venice Lagoon: (a) 6 m deep pole in salt marshes, CR0260; (b) anchoring on a preexisting shallow infrastructure, CR0610; (c) shallow concrete basement on embankments, CR0750; and (d) shallow foundation on steel network in salt marshes, CR0260a. Photos of (e) a TCR (CR0580) during high tides, (f) a TCR (CR0500) filled with debris, and (g) a damaged TCR (CR0640).

isles (known as "motte"), and along the banks bounding the fish farms within the Venice Lagoon and at the lagoon margins (Figure 1 and Table 1). The TCR network was planned taking into account the location of previously identified PTs in a ERS SAR interferometric analysis [*Teatini et al*., 2005; *Teatini et al*., 2007] and keeping to a value of about 1 km the maximum distance between the TCRs or between an "artificial" and the adjacent "natural" reflectors detected on the ERS SAR analysis. The TCRs are characterized by 60 cm edge length and made of aluminum to reduce their weight. They were usually installed in areas without other strong scatterers, on foundations at various depths (Figures 2a–2d), and at the same height above ground in order to study possible differences in their relative settlement. In salt marshes, which tend to sit at elevations between mean and high tide [*Silvestri et al*., 2005] and are thus visible through at least half of the tidal cycle of about ±50 cm [*Umgiesser and Matticchio*, 2006], the TCRs were installed

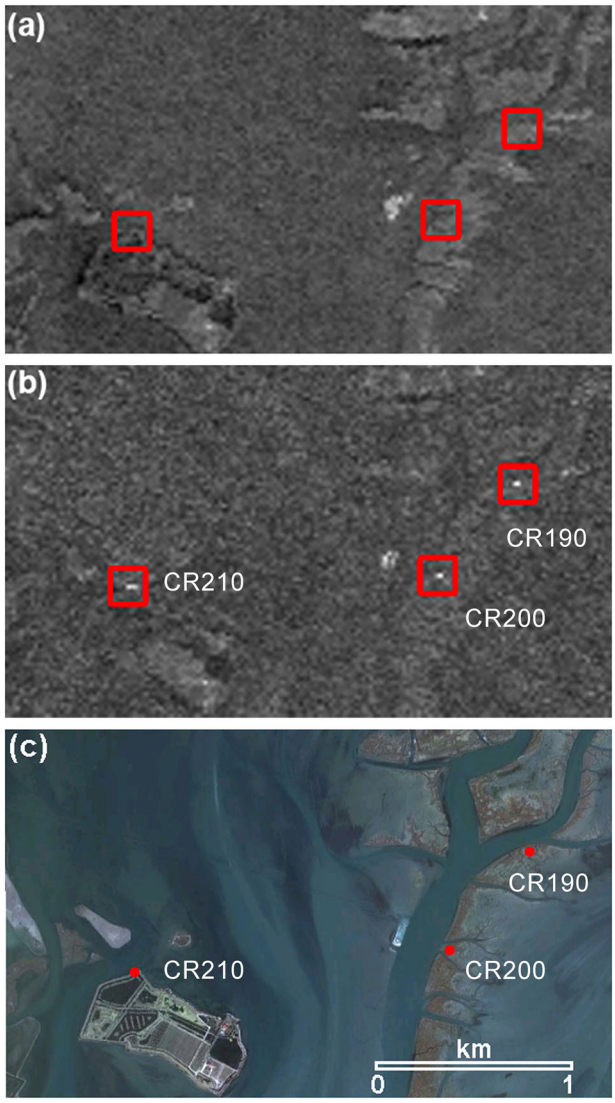

Figure 3. ENVISAT ASAR backscattering intensity image of a portion of the northern lagoon obtained by averaging the scenes acquired (a) before and (b) after September 2006. The locations of the TCRs are highlighted by the red boxes in Figures 3a and 3b, and by the red dots in the Landsat image shown in Figure 3c.

at a height of 1 m above the mean sea level to ensure that they are never flooded (Figure 2e). The radar reflectors were aligned with the satellite illumination following the instructions given by *Ge et al*. [2001]. Although primarily the set up to be used with ENVISAT IS2 acquisitions from a descending orbit with an incidence angle of ~23°, the TCRs are also clearly visible in TerraSAR-X stripmap images acquired along descending orbits with an incidence angle of ~30°. The ENVISAT ASAR images cover the time period from 2 April 2003 to 22 September 2010 with a nominal interval of 35 days between acquisitions. In general, the number of ENVISAT ASAR acquisitions over the TCRs varies between 30 and 40, depending on the TCR deployment date. Between 5 March 2008 and 29 August 2011, a total of 90 TerraSAR-X images were acquired with a nominal repetition time interval of 11 days.

[8] In order to locate the TCRs on the satellite radar images, the pixels corresponding to the TCRs in the SAR geometry were first computed using their geographic coordinates measured in situ and the satellite orbital information. After having confirmed their visibility on one SAR intensity image (Figure 3), the exact point target location at subpixel accuracy was determined by searching for the location of the intensity maximum in every radar image. The normalized backscatterer intensities extracted for ENVISAT ASAR and TerraSAR-X acquisitions as a function of range and azimuth for a TCR installed in a region that is lacking strong natural scatterers are presented in Figures 4a and 4b and in

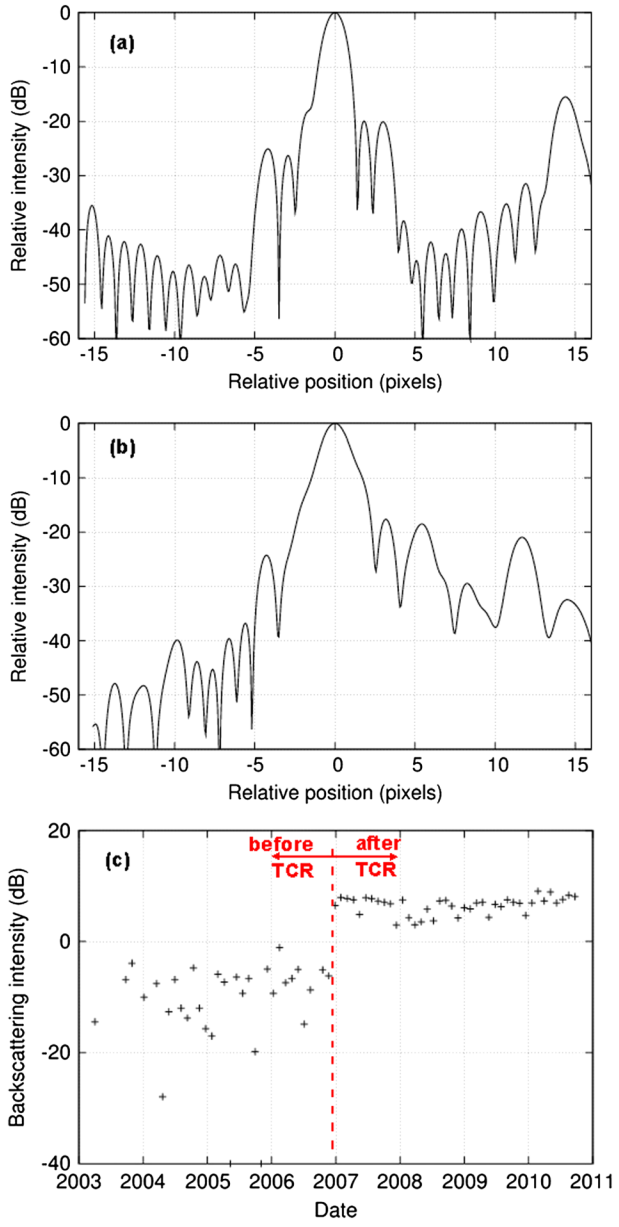

Figure 4. Normalized intensity as a function of (a) range and (b) azimuth for one ENVISAT ASAR acquisition, and (c) backscattering intensity as function of the acquisition time for CR0210. The time of TCR establishment is highlighted in Figure 4c.

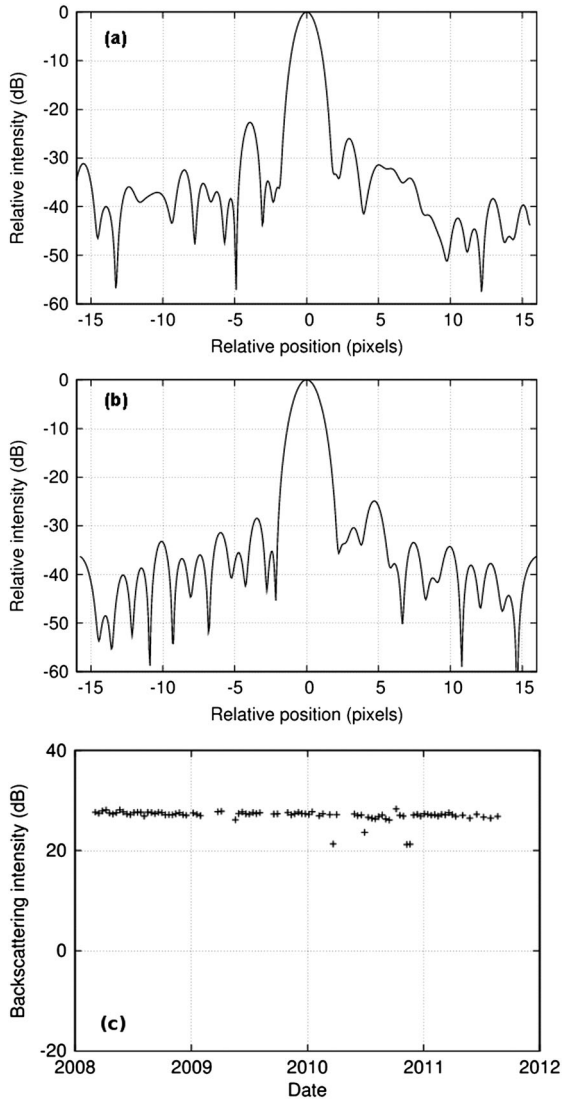

Figure 5. Normalized intensity as a function of (a) range and (b) azimuth for one TerraSAR-X acquisition, and (c) backscattering intensity as function of the acquisition time for CR0210.

Figures 5a and 5b, respectively. They show signal-to-clutter ratios (SCRs) better than 15 dB for ENVISAT and better than 25 dB for TerraSAR-X. The backscatterer intensity of the TCRs as a function of time was also analyzed. This is remarkably stable for the TerraSAR-X acquisitions (Figure 5c) and noisier for the ENVISAT ASAR scenes (Figure 4c), as consequence of the different wavelengths and resolutions of the two sensors with respect to the size of the TCRs and the background clutter. The SCR can be also estimated from the ratio of the amplitude standard deviation σ_a and mean m_a of the backscatterer amplitude as a function of time [*Adam et al*., 2005]:

$$\mathrm{SCR} = \frac{1}{2} \cdot \frac{\sigma_a^2}{m_a^2} \tag{1}$$

[9] For the 60 cm long TCRs, the SCR is generally on the order of 10 dB for ENVISAT and better than 25 dB for TerraSAR-X. From the analysis of the backscatter intensity as a function of time, it is also possible to investigate if a TCR was damaged (Figure 2g) or stolen. This happened for 19 TCRs, which were only partly replaced. A report on the TCR condition was prepared monthly after each ENVISAT acquisition and sent to the Venice Water Authority to implement appropriate countermeasure. In addition, we noticed a sudden drop of the backscattering intensity for a short period of time (one to a few SAR acquisitions) over some of the TCRs. We think that this is due to the presence of water into the reflectors when the hole at the bottom of the structure was filled with debris (e.g., eggs or leaves; see Figure 2f).

3. SAR Interferometry on the TCRs

[10] Having determined with subpixel precision the position of every TCR for every SAR acquisition, the complex backscattering values (intensity and phase) were extracted, and interferograms were computed with reference to a single master scene. According to the phase model, contributions in the interferograms are expected from the line of sight (LOS) displacement, the heights of the TCRs, and atmospheric and orbital effects [*Bamler and Hartl*, 1998; *Rosen et al*., 2000]. By taking into account the height of the TCRs determined during their installation, using the orbital data to simulate the flat Earth contribution and ignoring in a first step the atmosphere, the relative phase difference of neighboring pairs of TCRs was computed. In most of the cases, the interferometric phase showed an excellent relationship with time, and no displacement was observed. Only in a few examples was a clear subsidence trend visible.

[11] Our aim was however to include the TCR solution into the global interferometric analysis on natural persistent targets. In a typical PSI analysis, atmospheric and orbital effects are accurately estimated [*Werner et al*., 2003]. These data were therefore interpolated at the TCR positions. In the case of strongly varying regional atmospheric conditions—as observed in particular during the summer—interpolation in areas without natural reflectors can be inaccurate. This problem is particularly severe in the case

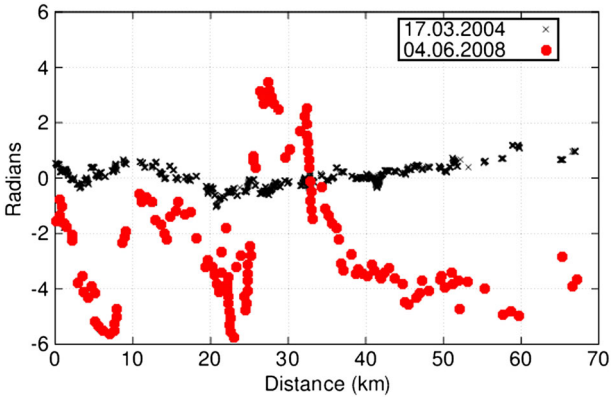

Figure 6. Phase signals attributed to atmospheric residuals in PSI for ENVISAT ASAR data as a function of the distance for a profile going from north to south at the western lagoon edge for an extremely turbulent summer situation (4 June 2008) and a typical winter stable condition (17 March 2004).

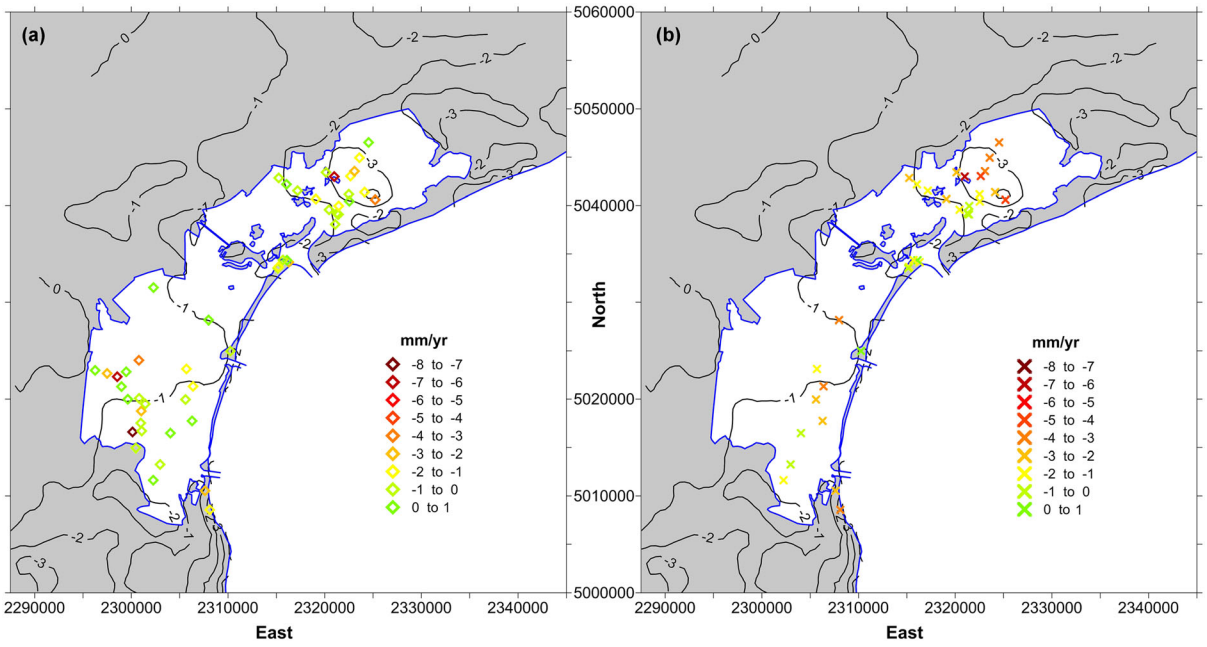

Figure 7. Average displacement rate (mm/yr) in the LOS direction on the TCR network measured with (a) ENVISAT ASAR and (b) TerraSAR-X data in the Gauss-Boaga reference frame. The black isolines represent the mean regional displacements from 2003 to 2010 obtained by interpolating the ENVISAT ASAR PSI measurements provided in Figure 1a using the kriging technique. Negative values mean land subsidence.

of ENVISAT. For TerraSAR-X, on the other hand, the density of natural point targets into the lagoon is remarkable. In addition, the solution of most of the TCRs is already included into the global interferometric point target analysis, because most of the TCRs were already installed when the acquisitions of TerraSAR-X began. After having applied the atmospheric corrections, the same reference point used for the global interferometric point target analysis was used also for the TCRs. As a further improvement, we changed the height of the TCRs because the reference point selected in the global solution was not at ground level. At the end, the time series of the unwrapped interferometric phases as a function of time (i.e., acquisition) were transformed to displacements.

4. Error Analysis

[12] The error in the measurement of the TCR displacement comes mainly from signal noise and uncompensated atmospheric path variation [*Hanssen and Feijt*, 1997]. The effective displacement error of a radar scatterer related to the signal noise, $r_{\mathrm{err}}^{\mathrm{SCR}}$, can be estimated from the SCR and the sensor wavelength λ by [*Adam et al.*, 2005]:

$$r_{\mathrm{err}}^{\mathrm{SCR}} = \frac{\lambda}{4} \cdot \frac{1}{\sqrt{2 \cdot \mathrm{SCR}}} \tag{2}$$

[13] By considering SCR values of 10 dB for ENVISAT and of 25 dB for TerraSAR-X (see section 3 for details), $r_{\mathrm{err}}^{\mathrm{SCR}}$ is 3.0 mm for ENVISAT and 0.3 mm for TerraSAR-X for TCRs with a 60 cm edge length.

[14] The turbulent behavior of masses of air causes a constant mixing leading to variations in temperature, pressure, and relative humidity, even at sub-kilometer scale. Horizontal temperature gradients, changes of relative humidity, and pressure changes have therefore considerable influence on the corresponding phase signals. In the PSI analysis, the atmospheric delay is estimated and subtracted for every point and each epoch. The quality of the atmospheric estimation strongly depends on the spatial sampling, with better estimates where there is high point density. If the TCRs are not yet included in the PSI solution, then extrapolation of the atmospheric delay will introduce an additional error. In Figure 6, the phase signals attributed to atmospheric residuals in PSI are plotted for ENVISAT ASAR data as a function of the distance for a profile going from north to south at the western lagoon edge in the case of an extremely turbulent summer situation (4 June 2008) and of typical stable winter conditions (17 March 2004). At distances of about 1 km, the variance of the atmospheric residual is at C band typically on the order of $\pi/4$, which corresponds to an atmospheric displacement error $r_{\mathrm{err}}^{\mathrm{ATM}}$ of 3.5 mm. Assuming that the spatial sampling of the TerraSAR-X and ENVISAT scatterers is identical, we would expect for TerraSAR-X the identical atmospheric displacement error as for ENVISAT. For TerraSAR-X, however, the density of natural point targets into the lagoon is much higher, resulting in a better estimation of the atmospheric residuals. Furthermore, the TCRs for TerraSAR-X were already part of the network used to estimate the atmospheric delay. We may thus assume in the case of TerraSAR-X a variance of the atmospheric residual on the order of $\pi/8$, which corresponds to an atmospheric displacement error $r_{\mathrm{err}}^{\mathrm{ATM}}$ of 1.0 mm.

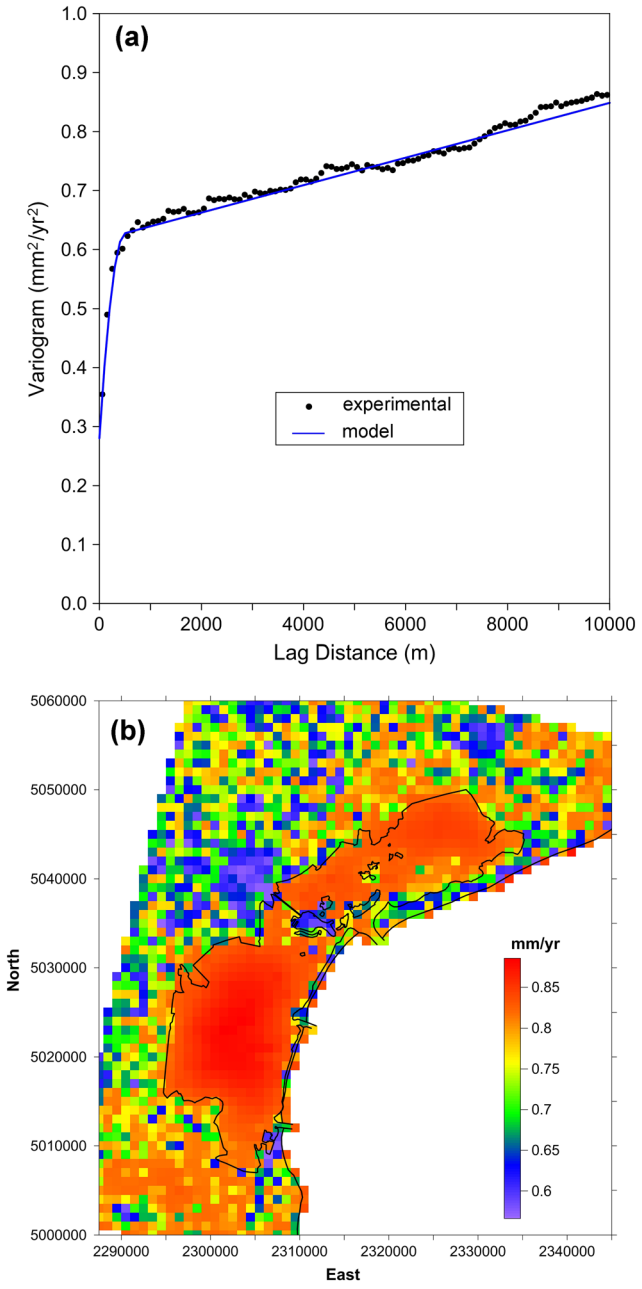

Figure 8. (a) Experimental variogram based on the displacement rates produced by PSI in the Venice region over the 2003–2010 period using ENVISAT ASAR data and model variogram fitted to the experimental one and used by the kriging interpolation technique. (b) Map of the standard deviation (mm/yr) computed by kriging and associated to the regional movement of Figure 7. Interpolation is performed on a regular 1×1 km grid. The model variogram takes the expression $\gamma = 0.28 + 2.33 \times 10^{-5} d + 0.336 \times (2d - d^2)$ for d 500 m and $\gamma = 0.616 + 2.33 \times 10^{-5} d$ for $d \geq 500$ m, with d the lag distance in [m]. The jump of the variogram at the origin, which is referred to as "nugget effect" and is suggested by the fitting of the experimental data, accounts for short-scale variability and inherent data incoherence.

[15] The error of a single measurement is computed as follows:

$$r_{\mathrm{err}} = \sqrt{\left(r_{\mathrm{err}}^{\mathrm{SCR}}\right)^2 + \left(r_{\mathrm{err}}^{\mathrm{ATM}}\right)^2} \tag{3}$$

[16] We obtain values of 4.6 mm for ENVISAT ASAR and of 1.0 mm for TerraSAR-X. The error of the mean velocity estimated with 40 ENVISAT ASAR images over a period of 3 years is then 0.3 mm/yr (i.e., $\left(4.6/\sqrt{40}\right)/3$). The error of the mean velocity estimated with 90 TerraSAR-X images over a period of 3 years is 0.1 mm/yr (i.e., $\left(1.0/\sqrt{90}\right)/3$).

[17] In order to increase the broad acceptability of SAR interferometry on persistent scatterers, a validation exercise with leveling and robotic tachymeters that addressed key issues, like quality assessment, performance assessment, and estimation of precision and accuracy, was performed in the past [*Crosetto et al.*, 2009]. For ENVISAT ASAR data, the average root-mean-square errors of single deformation measurements ranged between 4.2 and 6.1 mm, and the absolute standard deviation of the double difference in the rate of subsidence ranged from 1.0 to 1.8 mm/yr for a maximum subsidence rate of about 4 mm/yr over a time period of 5 years. These numbers are in good agreement with those computed before based on the TCRs data used in our experiment and can be used as error estimates in the discussion of our results, in particular for those TCRs that are not too isolated from natural point targets.

[18] These values must be evaluated in relation to the rates of sea level rise and land subsidence in our area of interest. In Venice, the average eustatic rise of the mean sea level over the last 120 years was quantified in 1.2 mm/yr [*Carbognin et al.*, 2004; *Carbognin et al.*, 2010]. Land subsidence is affecting the northern and southern basins of the Venice Lagoon, i.e., where the TCRs are located, at rates ranging between 1 and 4 mm/yr [*Teatini et al.*, 2005; *Tosi et al.*, 2010]. Hence, the accuracy of SAR interferometry on TCRs appears appropriate to quantify the processes of interest in the Venice area, in particular using X band scenes.

5. Results

5.1. Regional Versus TCR's Displacements

[19] The average displacement rate of the TCRs computed with the ENVISAT ASAR acquisitions covering the operational time interval is shown in Figure 7a. Only the TCRs for which at least 16 ENVISAT ASAR acquisitions are available are shown, not considering therefore the TCRs that were stolen or damaged shortly after their deployment (Table 1). In most of the cases, the displacement rate is smaller than about −2 mm/yr, and only for one TCR in the north of the lagoon (CR0210) and two other TCRs (CR0520 and CR0590) in the southern lagoon we did observe subsidence rates larger than 5 mm/yr.

[20] The TCR movements are compared with the regional land displacements characterizing the Venice coastal zone, i.e., the 80 km long and 30 km wide coastal area shown in Figure 1a. The isolines of subsidence rate used as reference in Figure 7 are obtained by filtering and interpolating the 2003–2010 ENVISAT ASAR PSI solution computed on

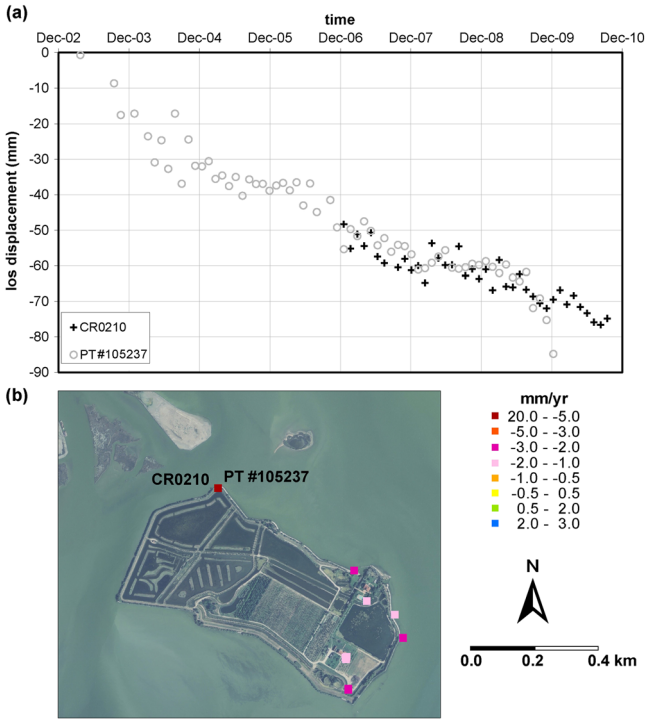

Figure 9. (a) Time series of LOS displacements obtained on ENVISAT ASAR images for CR0210 and the nearby natural PT #105237. (b) Location of the natural and artificial radar reflectors in the Santa Cristina Island. The colors are representative of the average movement rates from 2003 to 2010.

the natural PTs. Therefore, they are representative of land subsidence at regional scale due mainly to tectonics of the pre-Quaternary basements, a major presence of compressible clayey Quaternary deposits in the southern and northern portions of the study area, and groundwater withdrawals in the northeastern coastal region [*Tosi et al.*, 2009]. Filtering is carried out to remove significant changes of the measured displacements for adjacent PTs that are due to local causes, such as the variability of the Holocene deposits, the various depths of reference of the displacements due to the different types/depths of PT's foundations, and possible instabilities of different portions of the same structure [*Tosi et al.*, 2009; *Teatini et al.*, 2012]. To achieve this, a geostatistical technique using a spatial autocorrelation model characterized by the presence of a "nugget effect" [*Cressie,* 1991] is applied. Figure 8a provides the experimental variogram based on the PT's displacement and the model variogram that, fitted to the experimental one, has been used by kriging to interpolate the PT's movement rates and create the map shown in Figure 7. The displacement rate is assumed to be an isotropic stochastic variable satisfying the intrinsic hypothesis [*de Marsily,* 1986]. Kriging itself also provides an evaluation of the accuracy associated to the interpolated through the standard deviation (Figure 8b).

[21] The TCR displacement rates obtained by ENVISAT ASAR (Figure 7a) substantially match the regional land subsidence ranging between 1 and 3 mm/yr, taking also into consideration the reliability of the interpolated regional values within the lagoon, where the standard deviation is ~1 mm/yr. Exceptions are seen for CR0210, CR0520, and CR0590 that are settling faster. The possible reasons of these anomalies were investigated. Figure 9a compares the displacements of CR0210 and a nearby natural PT. The behaviors of the two radar reflectors are substantially similar, confirming the reliability of the PSI analysis on the artificial TCRs. As shown in Figures 1a and 9b, CR0210 was established on an embankment protected by stones of the Santa Cristiana Island. Therefore, the large subsidence rate is related to the local consolidation due to the surficial load. A similar situation characterizes CR0520 (Figure 10) that was founded on a bank bounding a fish farm in the southern portion of the lagoon.

[22] Especially interesting is the condition of CR0590. Figure 11 shows the displacement over time recorded by this TCR and by CR0600, which is located only 1 km farther east (Figure 1a) on a similar marshland environment. If the former is subsiding at more than 7 mm/yr, the latter is comparatively stable (Figure 7a and Table 1), both being founded on piles at approximately 6 m depth. Information concerning the morphological interventions carried out over the last two decades to contrast the deterioration of the lagoon environment indicates that CR0590 was installed in an artificial marshland built approximately 15 years ago. Conversely, the other stable TCRs in their surroundings (including CR0600) are placed on natural salt marshes. Therefore, the load of the artificial deposits on the compressible Holocene sediments is likely responsible for the recorded subsidence.

5.2. ENVISAT Versus TerraSAR-X Displacements of TCRs

[23] Although originally established for ENVISAT ASAR acquisitions, the TCRs are also visible in TerraSAR-X scenes. However, the several reflectors in the southwesternmost portion of the study area are outside the TerraSAR-X frame processed in this study. Figure 7b shows the average 2008–2011 subsidence rates detected on the TCRs using TerraSAR-X images. The values compare satisfactorily with the regional

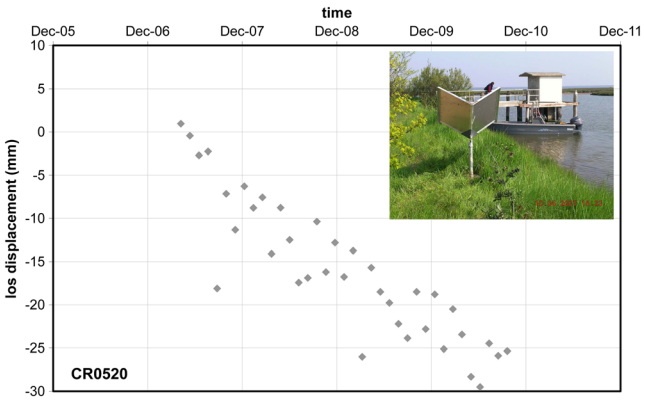

Figure 10. Time series of LOS displacements obtained on ENVISAT ASAR images for CR0520. The TCR is established by a surficial foundation on an embankment bounding a fish farm. A photo of the TCR is provided in the inset.

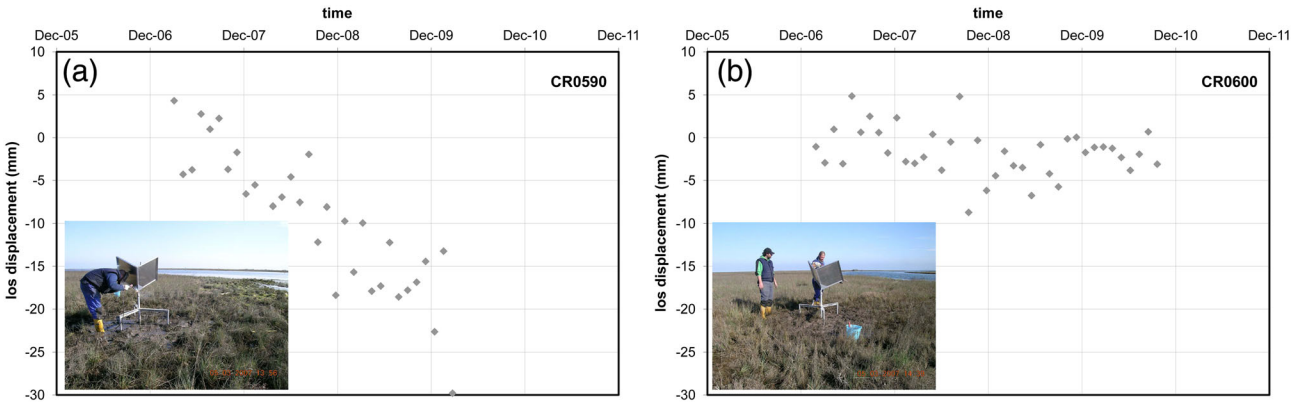

Figure 11. Time series of LOS displacements obtained on ENVISAT ASAR images for (a) CR0590 and (b) CR0600 established on an artificial and natural salt marsh, respectively. A photo of each TCR is provided in the inset.

trend, even better than ENVISAT ASAR in the northern sector of the lagoon where the largest regional land subsidence up to 3 mm/yr has been estimated over the period between 2003 and 2010.

[24] A more quantitative comparison between the TCR movements measured using ENIVSAT ASAR and TerraSAR-X acquisition is provided in Figure 12. The average displacement rate and the standard deviation associated with the mean are shown for the TCRs, where data from both satellites are available. Note the general good agreement between the two data sets. As expected, the noise is smaller with TerraSAR-X than with ENVISAT ASAR, with standard deviations of about 0.1 and 1 mm/yr, respectively. This is due to the better signal-to-clutter ratio of TerraSAR-X because the TCRs have higher radar cross section at X band and the background clutter is lower due to the smaller size of the radar image samples. The response between ENVISAT ASAR and TerraSAR-X differs significantly only for a few TCRs (CR0110, CR0150, CR0630, CR0720, and CR0730); these are those characterized by a large standard deviation. Inspection of Table 1 reveals that these TCRs remained active during a short period and, therefore, were detectable in a small number of images. Consequently, the interferometric processing is intrinsically less reliable. Figure 13 shows the displacement versus time for four TCRs detected using data from both satellites. The ENVISAT ASAR signal is noisier than TerraSAR-X and this can be seen for both subsiding (e.g., CR0210) and stable reflectors (e.g., CR0260).

[25] Differences between the average displacements for the two satellites are due partially to the nonoverlapping time intervals. An example is shown in Figure 13c that shows the displacements of CR0700. Note that the larger subsidence rate obtained by TerraSAR-X (3.1 mm/yr against 1.7 mm/yr by ENVISAT; Table 1) is mainly due to movements measured after mid-2008. The average displacement rates over the overlapping interval (from March 2008 to September 2010) amount to −2.74 and −2.70 mm/yr with ENVISAT and TerraSAR-X, respectively.

[26] The effect of the atmospheric interpolation within the lagoon is visible in the different level of noise for some of the TCRs. Clear evidence is obtained by comparing the displacements measured for CR0210 (Figure 13a) and CR0810 (Figure 13d), the former situated on an island within the lagoon more than 1 km far from any PTs, the latter in the urbanized Lido littoral. In general, if a TCR is not surrounded by natural reflectors, the ENVISAT ASAR analysis leads to an increased noise because the extrapolation of the atmosphere must be done using a larger radius. For TerraSAR-X, on the other hand, the standard PSI analysis already includes the TCR as a "natural" reflector because the acquisitions started when they were already deployed, and extrapolating the atmosphere near an isolated point effectively results in deviations from a linear model being classified as atmospheric variation. The noise of the TerraSAR-X series for TCRs established in urban zones is generally larger than in the case of the TCRs installed in a natural environment due to the lower level of clutter.

[27] Finally, a small monitoring network to validate the PSI measurements on the TCRs has been installed at the northern tip of the Lido littoral. Five TCRs were connected by high precision leveling surveys that were performed a few times during our experiment (Figure 14, top panel). Two examples of the displacements between CR0820 and CR0840 relative to CR0810 are shown in Figures 14a and 14b, respectively. In all the cases, the

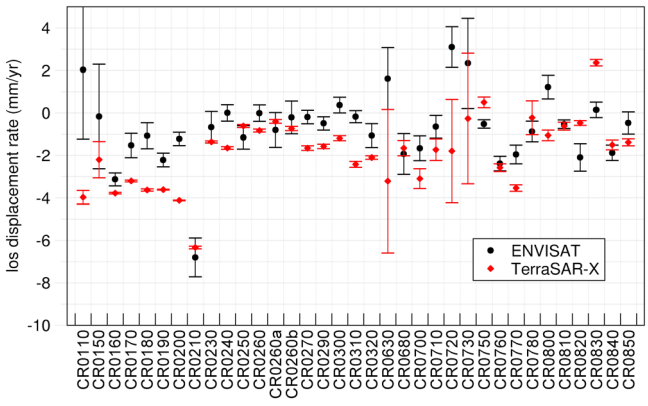

Figure 12. Comparison between the average LOS displacement rates computed by PSI over the 2003–2010 and 2008–2011 intervals using ENVISAT ASAR and TerraSAR-X acquisitions, respectively. The standard deviation associated to the mean is also shown.

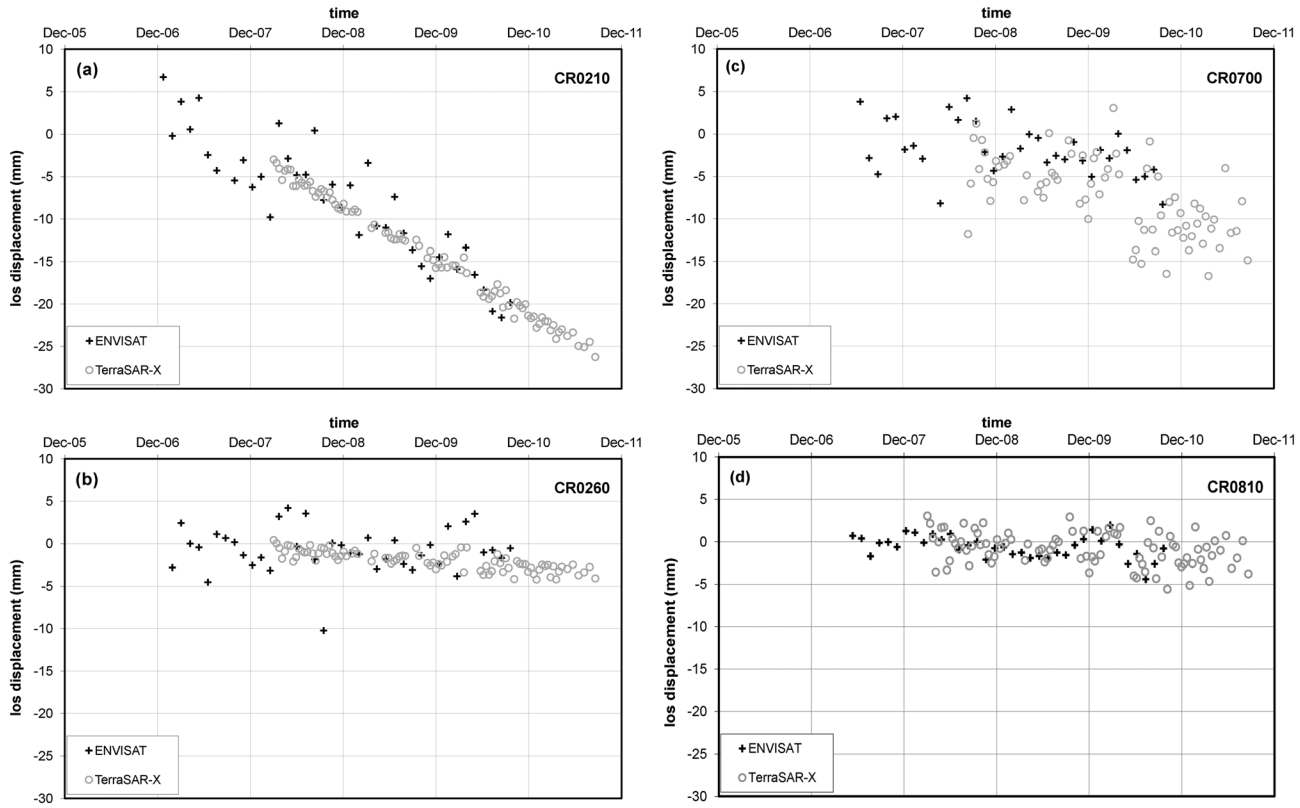

Figure 13. Time series of LOS displacements for (a) CR0210, (b) CR0260, (c) CR0700, and (d) CR0810 using ENVISAT ASAR (plus sign) and TerraSAR-X (open circle) data.

displacement rates are very small, ranging from −1.6 to +0.2 mm/yr and comparable to the errors associated to the TCR mean velocity discussed in section 4. For the single measurements, we observe values scattered within ±5 mm for ENVISAT and ±2 mm for TerraSAR-X with respect to the leveling surveys which are characterized by an accuracy of about ±0.5 mm.

6. Discussion

[28] Our experiment provided new information in order to improve the knowledge of the processes acting in the Venice Lagoon. We found that the northern basin of the lagoon is subsiding at a rate of about 3–4 mm/yr, while the central and the southern lagoon regions are more stable. Although these displacement trends detected on the TCRs substantially agree with the pattern of the subsidence components investigated at the scale of the whole Venice coast region [*Tosi et al*., 2009; *Bock et al*., 2012], this experiment provides for the first time a direct and reliable quantification of the marshland subsidence. In the past, the subsidence of the inner lagoon was only estimated by interpolating the leveling [*Carbognin et al*., 2004] and/or PT measurements recorded along the lagoon margin and in a few islands [*Teatini et al*., 2005; *Tosi et al*., 2009; *Tosi et al*., 2010].

[29] At the local scale, i.e., the scale of the single salt marshes, a significant difference between the regionally interpolated displacements and the TCR's movements has been detected in some cases. An example is related to the San Felice site, one of the tidal salt marshes studied in the past [e.g., *D'Alpaos et al*., 2007; *Marani et al*., 2013] and where CR0260, CR0260a, and CR0260b were established (Figure 1a). Being located at a short distance (500–1000 m) from the Cavallino littoral, the subsidence obtained through interpolation was estimated at rates from 2 to 3 mm/yr. However, the TCR measurements proved that the actual subsidence rate is less than 1 mm/yr (Table 1). This low subsidence is supported by the preservation of the marsh original morphological characteristics over the last decades [*Rizzetto and Tosi*, 2011]. The knowledge of the actual subsidence rate assumes a key role in the evolution of transitional environments. Land subsidence (relative to the mean sea level) is one of the most important factors controlling the fate of the tidal landforms as highlighted by the results of coupled physical-biological models [e.g., *Marani et al*., 2007; *Carniello et al*., 2009].

[30] Only a few TCRs are characterized by large subsidence rates. However, these conditions are representative of local processes such as consolidation of shallow lagoon subsoil due to man-made surficial loads like artificial marshes and embankments. This is confirmed by the establishment at different foundation depths of three TCRs in the San Felice site, a natural silty-sandy marsh grown on a pre-Roman sandy beach deposit. CR0260, CR0260a, and CR0260b are only few meters apart from one another (i.e., the subsoil can be assumed the same) and are founded at 4, 2, and 0.3 m depth below the ground surface, respectively. The similar subsidence rates measured for the three TCRs show that the shallow component of land subsidence caused by the consolidation of the recent deposits due to their own weight is

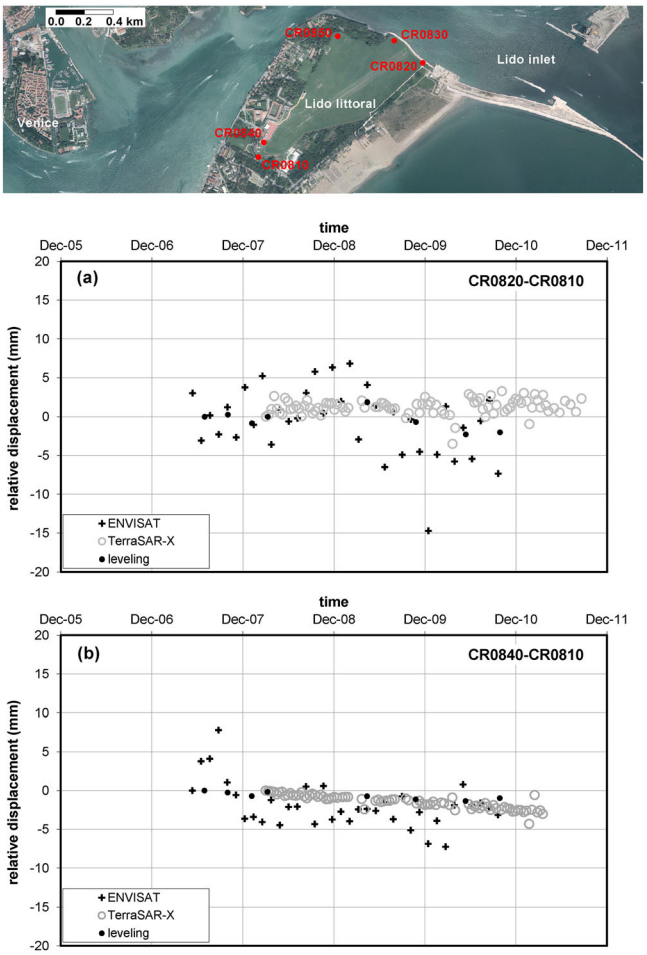

Figure 14. Time series of displacements for (a) CR0820 and (b) CR0850 relative to CR0810 using ENVISAT ASAR (plus sign) and TerraSAR-X (open circle) data. The leveling measurements are also shown (filled circle). The location of the Lido validation network is shown in the top map.

generally negligible. This does not occur where the lagoon bottom is loaded by large and heavy structures, such as embankments or artificial marshes.

[31] The relatively high subsidence rates measured in artificial marshes are particularly important for assessing the sustainability of these areas. In fact, tidal marshes are sustained vertically by plant growth and sedimentation that tends to maintain marsh plain elevations within a narrow band of the high intertidal range [*Fagherazzi et al.*, 2012]. The long-term sustainability of a marsh at any given site depends on the relative rates of sea level rise, plant productivity, sediment deposition, and subsidence, which interact to maintain the marsh elevation in a dynamic equilibrium with tide levels [*Orr et al.*, 2003].

[32] The subsidence rates measured by the TCRs on the lagoon marshes are an order of magnitude smaller than those that have characterized the evolution of the ground elevation of the farmland at the southernmost margin of the lagoon. These catchments were progressively reclaimed from marshland starting from the end of the nineteenth century and ending in the late 1930s. As a result, the area was turned into a fertile organic-rich farmland, kept dry by a distributed drainage system that collects the water from a capillary network of ditches and pumps it into the lagoon. Oxidation of peat started when aerobic conditions were established. Drainage of the outcropping peat soil, together with annual plowing, systematically brought poorly decomposed peat to the surface, resulting in subsidence rates of up to 30 mm/yr during the last 70–80 years [*Gambolati et al.*, 2005; *Zanello et al.*, 2011]. Where water-logged conditions persist, as in the marshes within the lagoon, oxidation of the organic matter is essentially precluded and does not contribute to present subsidence.

[33] A preliminary investigation has been performed in order to detect a possible correlation between the seasonal mean sea level fluctuation and short term TCR oscillations. The former is on the order of 700 mm between summer and winter at the tide gauge in Venice. The latter ranges between 4 and 10 mm (e.g., Figure 13b). In contrast to the analysis of *Teatini et al.* [2007] for natural reflectors, a relationship is not clearly observed in our case. Further investigation combining tide measurements and piezometric levels recorded in the proximity of the TCRs can possibly provide a more reliable answer to this issue.

[34] Given the potential of the technique to permit measurements in other similar settings, some general considerations and inherent limitations are formulated. From a methodological point of view, algorithms for processing satellite SAR data on TCRs are established. We found that 60 cm TCRs were sufficient for our investigations in areas lacking any strong scatterers, but that larger TCRs would improve the quality of the signal particularly at C band. In order to reduce size, cost of materials and air drag of the artificial reflectors, alternative designs, such as pentagonal corner reflectors [*Riechmann et al.*, 2011] or holed plates, [*Qin et al.*, 2013] can be considered. An important advantage of trihedral corner reflectors is their wide angular coverage. The 3 dB angular beam width of the TCRs is about 40°, and hence the same TCRs can be used for different SAR sensors illuminating the area of interest along similar orbital geometries (ascending or descending) but with different incidence angles, as is the case for TerraSAR-X and ENVISAT. In our experiment, we considered various solutions for mounting the TCRs at different depths (Figure 2) in order to study differential settlements. In all the cases, it was necessary to ensure the perfect stability of the reflectors, which caused us an important effort during installation.

[35] A careful planning of the TRC network is also required. On the one hand, it is an advantage if TCRs of reduced size are installed in areas with low clutter so that their reflectivity is higher than that of the background. On the other hand, it is important that the distance between nearby TCRs and PTs is kept less than 1–2 km in order to minimize phase jumps and avoid phase ambiguities. Moreover, this permits reduction of atmospheric disturbances that can be quite large in the coastal environments where temperature gradients, changes of relative humidity, and pressure variations have considerable influence on the phase signals, mainly during the summer. The number of TCRs in a network or the number of PTs in the immediate vicinity of each TCR is not relevant because analysis is performed on pairs of points.

7. Conclusions

[36] Interferometric analysis of a network of TCRs installed within the Venice Lagoon was performed with ENVISAT ASAR and TerraSAR-X data. The TCRs were established between the end of 2006 and the beginning of 2007, and monitored over the following 4–5 years. The experiment can be viewed as the first tentative of monitoring ground displacement of the morphological features typical of natural transitional environments, such as salt marshes and tidal flats, where radar reflectors are usually lacking and the use of traditional techniques is challenging. The importance of reliably and accurately controlling the ground elevation of lagoons, deltas, and wetlands is increasing worldwide in view of the expected sea level rise due to global climate changes. For the specific case of the Venice Lagoon, the loss of elevation relative to the mean sea level is one of the main factors that are contributing to a strong environmental deterioration which consists of the deepening of tidal flats and the reduction of the salt marshes.

[37] The biggest challenges we experienced in performing our experiment were the effort to deploy the TCRs and the vandalism that gradually reduced the number of points in the network. The inherent advantages of the TCR approach are at the same time its disadvantages: a restricted number of points from which to derive change and LOS displacement time series. But there is better control on the location, density, and depth of the detected motion. Our results are of important interest to those researchers working on similar natural hazard areas with TSX archive data that is just now becoming available for many conventional surface process applications.

[38] **Acknowledgments.** This work was supported by Magistrato alle Acque di Venezia—Venice Water Authority (VWA) and Consorzio Venezia Nuova (CVN) through the INLET Project and partially developed within the RITMARE Flagship Project (CNR-MIUR), Action 2 (SP3-WP1). We thank Giuseppe Zambon and Andrea Vianello (ISMAR-CNR) for the leveling measurements at the Lido littoral collected within the LAGUNA Project funded by CVN. Morgan S.r.l., Venice, is kindly acknowledged for its valued contribution in establishing the TCR's network and Stefano Libardo (Thetis S.p.A., previously CVN) for his essential activity in obtaining the permission of installing the TCRs within the Venice Lagoon. TERRASAR-X data courtesy LAN0242 and COA0612, © DLR.

References

Adam, N., B. Kempes, and M. Eineder (2005), Development of a scientific permanent scatterer system: Modifications for mixed ERS/ENVISAT time series, in *Proceedings of the 2004 Envisat & ERS Symposium, Eur. Space Agency Spec. Publ., ESA SP-572*, paper 2C1–1.

Bamler, R., and P. Hartl (1998), Synthetic aperture radar interferometry, *Inverse Probl.*, *14*, R1–R54.

Bell, J. W., F. Amelung, A. Ferretti, M. Bianchi, and F. Novali (2008), Permanent scatterer InSAR reveals seasonal and long-term aquifer-system response to groundwater pumping and artificial recharge, *Water Resour. Res.*, *44*, W02407, doi:10.1029/2007WR006152.

Bock, Y., S. Wdowinski, A. Ferretti, F. Novali, and A. Fumagalli (2012), Recent subsidence of the Venice Lagoon from continuous GPS and interferometric synthetic aperture radar, *Geochem. Geophys. Geosyst.*, *13*, Q03023, doi:10.1029/2011GC003976.

Bürgmann, R., G. Hilley, A. Ferretti, and F. Novali (2006), Resolving vertical tectonics in the San Francisco Bay Area from permanent scatterer InSAR and GPS analysis, *Geology*, *34*(3), 221–224.

Carbognin, L., P. Teatini, and L. Tosi (2004), Relative land subsidence in the lagoon of Venice, Italy, at the beginning of the new millennium, *J. Mar. Syst.*, *51*(1–4), 345-353.

Carbognin, L., P. Teatini, A. Tomasin, and L. Tosi (2010), Global change and relative sea level rise at Venice: What impact in term of flooding, *Clim. Dyn.*, *35*, 1039–1047.

Carniello, L., A. Defina, and L. D'Alpaos (2009), Morphological evolution of the Venice lagoon: Evidence from the past and trend for the future, *J. Geophys. Res.*, *114*, F04002, doi:10.1029/2008JF001157.

Coulson, S., and J. Guignard (1994), SAR interferometry with ERS-1, in *Proceedings of the Second Euro-Latin American Space Days, Buenos Aires, Argentina, 9-13 May, 1994*, edited by N. Longdon, *Eur. Space Agency Spec. Publ., ESA SP-363*, pp. 135–139.

Cressie, N. (1991), Statistics for Spatial Data, John Wiley and Sons, New York.

Crosetto, M., O. Monserrat, C. Bremmer, R. Hanssen, R. Capes, and S. Marsh (2009), Ground motion monitoring using SAR interferometry: Quality assessment, *Eur. Geol.*, *26*, 12–15.

D'Alpaos, A., S. Lanzoni, M. Marani, and A. Rinaldo (2007), Landscape evolution in tidal embayments: Modeling the interplay of erosion, sedimentation, and vegetation dynamics, *J. Geophys. Res.*, *112*, F01008, doi:10.1029/2006JF000537.

de Marsily, G. (1986), Quantitative Hydrology: Groundwater Hydrology for Engineers, Academic Press, Inc., New York.

Fagherazzi, S., et al. (2012), Numerical models of salt marsh evolution: Ecological, geomorphic, and climatic factors, *Rev. Geophys.*, *50*, RG1002, doi:10.1029/2011RG000359.

Ferretti, A., C. Prati, and F. Rocca (2001), Permanent scatterers in SAR interferometry, *IEEE Trans. Geosci. Remote Sens.*, *39*(1), 8–20.

Ferretti, A., G. Savio, R. Barzaghi, A. Borghi, S. Musazzi, F. Novali, C. Prati, and F. Rocca (2007), Submillimeter accuracy of InSAR time series: Experimental validation, *IEEE Trans. Geosci. Remote Sens.*, *45*(5), 1152–1153.

Fu, W., H. Guo, Q. Tian, and X. Guo (2010), Landslide monitoring by corner reflectors differential interferometry SAR, *Int. J. Remote Sens.*, *31*(24), 6387-6400.

Gambolati, G., M. Putti, P. Teatini, M. Camporese, G. Ferraris, G. Gasparetto Stori, V. Nicoletti, F. Rizzetto, S. Silvestri, and L. Tosi (2005), Peatland oxidation enhances subsidence in the Venice watershed, *Eos. Trans. AGU*, *86*(23), 217–224.

Ge, L., C. Rizos, S. Han, and H. Zebker (2001), Mining subsidence monitoring using the combined InSAR and GPS approach, paper presented at 10th FIG International Symposium on Deformation Measurements, SPONSOR, International Federation of Surveyors (FIG), Orange, Calif.

Hanssen, R., and A. Feijt (1997), A first quantitative evaluation of atmospheric effects on SAR interferometry, in *Proceedings Fringe 96' Workshop on ERS SAR Interferometry* [CD-ROM], *Eur. Space Agency Spec. Publ., ESA SP-406.*

Ketelaar, V. B. H. (2009), *Satellite Radar Interferometry: Subsidence Monitoring Techniques, Remote Sens. and Digital Image Processing*, vol. 13, 243 pp., Springer.

Marani, M., A. D'Alpaos, S. Lanzoni, L. Carniello, and A. Rinaldo (2007), Biologically-controlled multiple equilibria of tidal landforms and the fate of the Venice lagoon, *Geophys. Res. Lett.*, *34*, L11402, doi:10.1029/2007GL030178.

Marani, M., C. da Lio, and A. D'Alpaos (2013), Vegetation engineers marsh morphology through multiple competing stable states, *Proc. Natl. Acad. Sci. U. S. A.*, *110*(9), pp. 3259–63, doi:10.1073/pnas.1218327110.

Marinkovic, P., V. B. H. Ketelaar, and R. Hanssen (2004), A controlled Envisat/ERS permanent scatterer experiment, implications of corner reflector monitoring, in *Proceedings of CEOS SAR Workshop*, paper 37, Publ. Div., Eur. Space Res. and Technol. Cent., Eur. Space Agency, Noordwijk, Netherlands.

Marinkovic, P., V. B. H. Ketelaar, F. van Leijen, and R. Hanssen (2008), InSAR quality control: Analysis of five years of corner reflector time series, in *Proceedings of FRINGE 2007 Workshop, Eur. Space Agency Spec. Publ., ESA SP-649*.

Morton, R. A., and J. C. Bernier (2010), Recent subsidence-rate reductions in the Mississippi Delta and their geological implications, *J. Coastal Res.*, *26*(3), 555–561.

Orr, M., S. Crooks, and P. B. Williams (2003), Will restored tidal marshes be sustainable?, *San Francisco Estuary and Watershed Sci.*, *1*(1). Retrieved from: http://www.escholarship.org/uc/item/8hj3d20t.

Qin, Y., D. Perissin, and L. Lei (2013), The design and experiments on corner reflectors for urban ground deformation monitoring in Hong Kong, *Int. J. Antennas Propag.*, 2013, 191685, 8, doi:10.1155/2013/191685.

Riechmann, B., S. Knospe, and W. Busch (2011), Deformation measurements with TerraSAR-X time series based on Corner Reflectors, paper presented at 4th TerraSAR-X Science Team Meeting, DLR (Deutsches Zentrum für Luft- und Raumfahrt), Oberpfaffenhofen, Germany, 14-16 Feb.

Rizzetto, F., and L. Tosi (2011), Aptitude of modern salt marshes to counteract relative sea-level rise, Venice Lagoon (Italy), *Geology*, *39*(8), 755–758.

Rosen, P., S. Hensley, I. Joughin, F. Li, S. Madsen, E. Rodriguez, and R. Goldstein (2000), Synthetic aperture radar interferometry, *Proc. Inst. Electr. Eng.*, *88*(3), 333–382.

Silvestri, S., A. Defina, and M. Marani (2005), Tidal regime, salinity and salt marsh plant zonation, *Estuarine Coastal Shelf Sci.*, *62*(1-2), 119–130, doi:10.1016/j.ecss.2004.08.010.

Strozzi, T., P. Teatini, and L. Tosi (2009), TerraSAR-X reveals the impact of the mobile barrier works on Venice coastland stability, *Remote Sens. Environ.*, *113*(12), 2682–2688.

Syvitski, J. P. M., et al. (2009), Sinking deltas due to human activities, *Nat. Geosci.*, *2*, 681–686.

Teatini, P., L. Tosi, S. Strozzi, L. Carbognin, U. Wegmüller, and F. Rizzetto (2005), Mapping regional land displacements in the Venice coastland by an integrated monitoring system, *Remote Sens. Environ.*, *98*(4), 403–413.

Teatini, P., T. Strozzi, L. Tosi, U. Wegmüller, C. Werner, and L. Carbognin (2007), Assessing short- and long-time displacements in the Venice coastland by synthetic aperture radar interferometric point target analysis, *J. Geophys. Res.*, *112*, F01012, doi:10.1029/2006JF000656.

Teatini, P., et al. (2011a), Geomechanical response to seasonal gas storage in depleted reservoirs: A case study in the Po River basin, Italy, *J. Geophys. Res.*, *116*, F02002, doi:10.1029/2010JF001793.

Teatini, P., L. Tosi, and T. Strozzi (2011b), Quantitative evidence that compaction of Holocene sediments drives the present land subsidence of the Po Delta, Italy, *J. Geophys. Res.*, *116*, B08407, doi:10.1029/2010JB008122.

Teatini, P., L. Tosi, T. Strozzi, L. Carbognin, G. Cecconi, R. Rosselli, and S. Libardo (2012), Resolving land subsidence within the Venice Lagoon by persistent scatterer SAR interferometry, *Phys. Chem. Earth*, *40-41*, 72–79, doi:10.1016/j.pce.2010.01.002.

Tosi, L., L. Carbognin, P. Teatini, T. Strozzi, and U. Wegmüller (2002), Evidence of the present relative land stability of Venice, Italy, from land, sea, and space observations, *Geophys. Res. Lett.*, *29*(12), 1562, doi:10.1029/2001GL013211.

Tosi, L., P. Teatini, L. Carbognin, and G. Brancolini (2009), Using high resolution data to reveal depth-dependent mechanisms that drive land subsidence: The Venice coast, Italy, *Tectonophysics*, *474*, 271–284.

Tosi, L., P. Teatini, T. Strozzi, L. Carbognin, G. Brancolini, and F. Rizzetto (2010), Ground surface dynamics in the northern Adriatic coastland over the last two decades, *Rend. Fis. Accad. Lincei*, *21*, suppl. 1, 115–129.

Umgiesser, G., and B. Matticchio (2006), Simulating the mobile barrier (MOSE) operation in the Venice Lagoon, Italy: Global sea level rise and its implication for navigation, *Ocean Dyn.*, *56*, 320–332, doi:10.1007/s10236-006-0071-4.

Vasco, D. W., A. Rucci, A. Ferretti, F. Novali, R. C. Bissell, P. S. Ringrose, A. S. Mathieson, and I. W. Wright (2010), Satellite-based measurements of surface deformation reveal fluid flow associated with the geological storage of carbon dioxide, *Geophys. Res. Lett.*, *37*, L03303, doi:10.1029/2009GL041544.

Werner, C., U. Wegmüller, T. Strozzi, and A. Wiesmann (2003), Interferometric point target analysis for deformation mapping, paper presented at International Geoscience and Remote Sensing Symposium 2003, Inst. of Electr. and Electron. Eng., New York.

Xia, Y., H. Kaufmann, and X. F. Guo (2002), Differential SAR interferometry using corner reflectors, paper presented at International Geoscience and Remote Sensing Symposium 2002, Inst. of Electr. and Electron. Eng., New York.

Xia, Y., H. Kaufmann, and X. F. Guo (2004), Landslide monitoring in the Three Gorges area using D-INSAR and corner reflectors, *Photogramm. Eng. Remote Sens.*, *70*(10), 1167–1172.

Zanello, F., P. Teatini, M. Putti, and G. Gambolati (2011), Long term peatland subsidence: Experimental study and modeling scenarios in the Venice coastland, *J. Geophys. Res.*, *116*, F04002, doi:10.1029/2011JF002010.